Title Page

Title: Age-Related Changes in Expression and Activity of Human Hepatic Mitochondrial Glutathione Transferase Zeta1

Authors: Guo Zhong, Margaret O. James, Marci G. Smeltz, Stephan C. Jahn, Taimour Langaee, Pippa Simpson and Peter W. Stacpoole

Department of Medicinal Chemistry (G.Z., M.O.J., M.G.S., S.C.J.), Pharmacotherapy and Translational Research (T.L.), Center for Pharmacogenomics (T.L.), and Departments of Medicine and Biochemistry and Molecular Biology (P.W.S.), University of Florida, Gainesville, Florida; Department of Pediatrics, Medical College of Wisconsin, Milwaukee, Wisconsin (P.S.)

Running title Page

Age-Related Development of Human Mitochondrial GSTZ1

Corresponding Author: Margaret O. James

Department of Medicinal Chemistry, University of Florida

Gainesville, FL 32610-0485

mojames@ufl.edu

Phone: 1 (352) 273-7707

Number of text pages: 22 (37 including all text, references and tables)

Number of figures: 11 (3 supplemental figures included)

Number of tables: 5

Number of References: 54

Number of words in *Abstract*: 250

Number of words in *Introduction*: 795

Number of words in *Discussion*: 1582

Abbreviations used:

ABC buffer, ammonium bicarbonate buffer; ACN, acetonitrile; DCA, dichloroacetate; GGT, gamma-glutamyl transpeptidase; GSTZ1, glutathione transferase zeta1; GSH; glutathione; IP, immunoprecipitation; LOQ, limit of quantitation; MSA, multistage activation; PBS-T, tween-20 in phosphate buffered saline; RT, room temperature; $t_{1/2}$, inactivation half-life; TFA, trifluoroacetic acid; Y, years of age.

Abstract

Glutathione transferase zeta1 (GSTZ1) catalyzes glutathione (GSH)-dependent dechlorination of dichloroacetate (DCA), an investigational drug with therapeutic potential in metabolic disorders and cancer. GSTZ1 is expressed in both hepatic cytosol and mitochondria. Here, we examined the ontogeny and characterized the properties of human mitochondrial GSTZ1. GSTZ1 expression and activity with DCA were determined in 103 human hepatic mitochondrial samples prepared from livers of donors aged 1 day to 84 years. DNA from each sample was genotyped for three common GSTZ1 functional single nucleotide polymorphisms. Expression of mitochondrial GSTZ1 protein increased in an age-dependent manner to a plateau after age 21 years. Activity with DCA correlated with expression, after taking into account the somewhat higher activity of samples that were homo- or heterozygous for GSTZ1A. In samples from livers with the GSTZ1C variant, apparent enzyme kinetic constants for DCA and GSH were similar for mitochondria and cytosol after correcting for the loss of GSH observed in mitochondrial incubations. In the presence of 38 mM chloride, mitochondrial GSTZ1 exhibited shorter half-lives of inactivation compared with the cytosolic enzyme ($p=0.017$). GSTZ1 protein isolated from mitochondria was shown by mass spectrometry to be identical to cytosolic GSTZ1 protein in the covered primary protein sequence. In summary, we report age-related development in the expression and activity of human hepatic mitochondrial GSTZ1 does not have the same pattern as that reported for cytosolic GSTZ1. Some properties of cytosolic and mitochondrial GSTZ1 differed, but these were not related to differences in amino acid sequence or post-translationally modified residues.

Introduction

Glutathione transferase zeta1 (GSTZ1), also known as maleylacetoacetate isomerase (MAAI), catalyzes the isomerization of maleylacetoacetate to fumarylacetoacetate, one of the reactions involved in the process of tyrosine degradation (Board and Anders, 2011). GSTZ1 is also responsible for biotransformation of α-haloacetic acids (Tong et al., 1998). Dichloroacetate (DCA) is converted to an inactive metabolite, glyoxylate, through glutathione (GSH)-dependent dechlorination by GSTZ1 (James et al., 1997). DCA is an investigational drug with potential clinical applications in treating cancer, cardiovascular and metabolic disorders (Stacpoole, 2011; Kankotia and Stacpoole, 2014; James et al., 2017). Its primary mechanism of action is to inhibit mitochondrial pyruvate dehydrogenase kinase thereby maintaining the pyruvate dehydrogenase complex in its unphosphorylated, catalytically active, form (Stacpoole et al., 1998). Pyruvate dehydrogenase complex functions as a key cellular homeostat in regulating mitochondrial fuel metabolism and oxidative phosphorylation. Repeated dosing of DCA causes slower clearance of the drug in both human and animals, resulting from the inactivation of GSTZ1 (James et al., 1998; Tzeng et al., 2000; Shroads et al., 2008). Inactivation of GSTZ1 leads to accumulation of DCA as well as the chemically reactive tyrosine catabolites maleylacetoacetate and maleylacetone (Lantum et al., 2003; Shroads et al., 2008), which are possibly related to DCA's toxicity, as they are known to form adducts (Lantum et al., 2002b). A better understanding of DCA metabolism is important for selecting appropriate doses for patients.

Several factors have been demonstrated to influence DCA metabolism, including GSTZ1 haplotype, age and liver chloride concentration. In the coding region of the human *GSTZ1* gene there are 3 common nonsynonymous functional single nucleotide polymorphisms (SNPs), namely rs7975 G>A (E32K), rs7972 G>A (G42R) and rs1046428 C>T (T82M). In populations studied to date, these SNPs result in 5 major haplotypes, as reviewed recently (James and Stacpoole, 2016). In order of frequency in populations studied to date these are EGT (GSTZ1C,

most common, 45-55%); KGT (GSTZ1B, 25-35%); EGM (GSTZ1D, 10-20%); KRT (GSTZ1A, 1-10%) and KGM (GSTZ1F, 0-2%). *In vitro* studies examining GSTZ1 activity with DCA in human liver cytosol showed that activity in cytosols from *GSTZ1A* carriers was about 3-fold higher than in those from livers carrying all the other variants (non-*GSTZ1A* carriers), although when samples from all ethnicities were compared, the expression levels of GSTZ1 protein among the variants were similar (Li et al., 2012). Other variants have been reported, but are very rare (Yang et al., 2017). In people, age affects DCA pharmacokinetics and toxicity. Chronic treatment with DCA results in a greater decrease in drug clearance in adults compared with children (Shroads et al., 2008). Adults are also more susceptible than children to peripheral neuropathy, the principal adverse side effect caused by chronic DCA treatment (Kaufmann et al., 2006; Stacpoole et al., 2008). Chloride, at a concentration of 38 mM, reported to be the mean concentration in four human liver samples (Widdowson and Dickerson, 1960), substantially extended half-lives of DCA-induced GSTZ1 inactivation in human liver cytosol samples through an as yet unknown mechanism (Zhong et al., 2014). The concentration of chloride that protected cytosolic GSTZ1 from inactivation was haplotype-dependent (Zhong et al., 2014). Further studies of the chloride concentration of human liver in 97 donors aged 1 day to 84 years showed the mean whole liver concentration was 42 mM, the chloride concentration in human liver cytosol averaged 105 mM, and exhibited an age-related decline, while mitochondrial chloride concentrations were lower, 4.2 mM, and increased slightly with age (Jahn et al., 2015).

GSTZ1 mRNA expression in humans was highest in liver among all tested tissues (Uhlen et al., 2015). Based on studies in rodents, the hepatic cytosol is the major protein expression site of GSTZ1 (Lantum et al., 2002a; Jahn et al., 2018). Aside from cytosol, GSTZ1 was expressed in the hepatic mitochondrial matrix in both humans and rats, but at a lower level compared with cytosol (Li et al., 2011). Previously, the ontogeny of human hepatic cytosolic GSTZ1 was studied in our laboratory (Li et al., 2012). It is not known if GSTZ1 expressed in human liver

5

mitochondria exhibits identical properties to the cytosolic form with respect to ontogeny, enzyme

kinetics, primary protein sequence and DCA-induced inactivation, as the mechanism for

mitochondrial incorporation of the enzyme is not clear. Considering that the mitochondrion is the

primary action site of DCA, and the further metabolism of glyoxylate to carbon dioxide and

glycine takes place there, mitochondria play an important role in DCA biotransformation (James

et al., 1998). A deeper understanding of mitochondrial GSTZ1 properties will improve our

understanding of the fate of DCA in people (James et al., 2017). In this study, we investigated

the developmental pattern of human GSTZ1 in liver mitochondria. We also tested the

hypothesis that mitochondrial GSTZ1 differs from cytosolic GSTZ1 in enzyme kinetics and

stability properties related to DCA-induced inactivation.

Methods and Materials

Chemicals and Reagents. An aqueous 2 mM solution of Na [1-^{14}C]-DCA, containing 10–

40 µCi/mL, was made by neutralizing [1-^{14}C]-DCA (56 mCi/mmol, 99% purity) purchased from

American Radiolabeled Chemicals (St. Louis, MO) with $NaHCO_3$ and then adding unlabeled

clinical grade NaDCA (TCI America, Portland, OR) to the desired concentration and specific

activity. All other chemicals and reagents used in this study were of American Chemical Society

grade or higher and were purchased from commercial suppliers.

Human liver samples. Normal human liver samples from 41 female and 62 male de-

identified donors, aged 1 day-84 years, were obtained from three tissue banks under an exempt

protocol reviewed and approved by the University of Florida Internal Review Board. The tissue

banks were the Cooperative Human Tissue Network, University of Alabama at Birmingham, the

NICHD Brain and Tissue Bank of the University of Maryland, and the University of Florida

Clinical and Translational Science Institute. Samples were processed into subcellular fractions

following published procedures (Li et al., 2011) and stored at -80 °C until use. DNA was isolated

from nuclear pellets for genotyping: following amplification by polymerase chain reaction,

hepatic DNA was pyrosequenced, targeting the three common nonsynonymous SNPs, G94>A, G124>A and C245>T (Li et al., 2012; Langaee et al., 2015). Genotyping analysis used a PSQ HS 96 system (Qiagen, Germantown, MD) and haplotypes computationally inferred from the unphased data (PHASE software, version 2.0.2, University of Chicago, IL). The protein concentration of subcellular fractions was measured by a Pierce bicinchoninic acid (BCA) protein assay kit (Thermo Fisher Scientific, Waltham, MA).

GSTZ1 activity assay with DCA. GSTZ1 activity with DCA in human liver mitochondria and cytosol was measured by published methods (Li et al., 2011). Human liver mitochondrial samples were placed on ice and sonicated for 10 seconds twice, with a 25-s interval, to disrupt the mitochondrial membrane. Sonicated mitochondria samples were then dialyzed against 1.15% KCl, 0.05 M potassium phosphate buffer (pH 7.4) to remove sucrose, shown previously to inhibit GSTZ1 activity. Assay tubes were incubated at 37 °C, with gentle shaking. The reaction mixture contained 0.4 - 0.9 mg dialyzed protein, 200 μM Na [1-14C]-DCA, 5 mM GSH and 0.1 M Hepes-NaOH (pH 7.6) in a total volume of 0.1 mL. The reaction was started by adding mitochondrial protein and vortex-mixing, and then stopped after 30 min by the addition of ice-cold methanol to precipitate protein. These conditions were saturating for DCA and GSH and were linear for product formation. After centrifugation, the amount of [14C]-glyoxylate formed in the filtered sample was determined by high-performance liquid chromatography with radiochemical detection. The enzyme activity is expressed as nmol glyoxylate/min/mg protein. For liver cytosol samples, samples were not sonicated; dialyzed protein of 0.05 – 0.1 mg and 1 mM GSH were used in the assay with 10 min incubation time.

To study enzyme kinetics, activity assays were performed, in which dialyzed samples of human liver cytosol or mitochondria (0.1-0.5 mg protein) were incubated with varying concentrations of GSH or [1-14C] NaDCA. To determine apparent kinetic constants for GSH, the concentration of NaDCA was 0.2 mM and 8 to 10 GSH concentrations between 0.001 and 5 mM were used. To determine apparent NaDCA kinetic constants, the GSH concentration was 5mM

7

(mitochondria) or 1 mM (cytosol) and 8 NaDCA concentrations varied between 5 and 200 µM.

Incubation times were 10 and 30 min for cytosol and mitochondria samples, respectively (Li et

al., 2012). GSTZ1 activity was measured as described above. All samples were assayed in

duplicate.

Measurement of GSH consumption. To determine the stability of GSH in liver cytosol or

mitochondria, human liver cytosol and sonicated mitochondria from adults age 31 to 45 were

dialyzed against 1.15% KCl, 0.05 M K-phosphate buffer (pH 7.4) using 10k MWCO filters

(Millipore, Billerica, MA), to remove GSH from these samples. The protein concentrations of the

dialyzed samples were measured by Bio-Rad protein assay. Dialyzed cytosol or mitochondria

samples, 300 µg protein, were incubated with varying concentrations of GSH (0.025 to 1 mM),

0.1 M Hepes-NaOH buffer (pH 7.6) and water in a total volume of 100 µL at 37°C with gentle

shaking. After 0 and 10 min (cytosol) or 0 and 30 min (mitochondria), 100 µL of ice-cold

methanol was added and tubes were centrifuged to precipitate protein. The GSH concentration

in the supernatant was measured by derivatization and fluorescence spectrophotometry based

on published methods (Hissin and Hilf, 1976). An aliquot of the supernatant, 0.012 to 0.12 mL

was incubated with 1 mL 0.1M potassium phosphate buffer pH 8 containing 0.005 M EDTA, 0.1

mL of 0.1% o-phthalaldehyde prepared in methanol, and water to a total volume of 2.5 mL at

room temperature for 20 min. Fluorescent intensity was measured by LS 55 Luminescence

Spectrometer (PerkinElmer, Waltham, MA) at excitation 350 nm and emission 420 nm. A

standard curve of known concentrations of GSH was used for quantitation. All samples were

measured in duplicate.

Gamma-glutamyl transpeptidase activity. A spectrophotometric assay was used to

determine γ-glutamyltranspeptidase (GGT) activity (Tate and Meister, 1977). Cuvettes

contained 1 mM L-γ-glutamyl-*p*-nitroanilide (Sigma Aldrich), 20 mM glycylglycine (Sigma

Aldrich) and 1 mg of human liver mitochondria or cytosol from adults age 31 to 45 in a total

volume of 2 mL 0.1 M Tris-HCl pH 8 at 37 °C. The absorbance at 410 nm was recorded each

minute for 1 h, and the linear change in absorbance between 1 and 30 min used to calculate the concentration of p-nitroaniline released using the published molar extinction coefficient of 8800 cm^{-1}.

Western blot. Known amounts of mitochondrial protein (40–200 µg) were used to develop blots, using a custom-prepared rabbit polyclonal antibody to human GSTZ1C (Li et al., 2012) together with a rabbit monoclonal antibody to a synthetic peptide corresponding to residues near the C-terminus of human ALDH1A1 (Abcam, Cambridge, MA), used as a marker of cytosolic contamination of the mitochondria. Both primary antibodies were diluted 1:2,000. The amount of mitochondrial protein (40-200 µg) loaded in the gel was guided by measured mitochondrial GSTZ1 activity with DCA. Each gel included 5 µg of a single designated human liver cytosol as a reference control. After the blot was visualized and digitized by Bio-Rad ChemiDoc^{TM} MP Imaging System (Bio-Rad Laboratories, Hercules, CA), the intensity of bands was analyzed by Image Lab software (Bio-Rad Laboratories, Hercules, CA). Standard curves for GSTZ1, monomeric molecular weight 25 kDa, were constructed using hGSTZ1C (Guo et al., 2006). To quantify test samples, the signal of each individual test sample was normalized against the reference control. The GSTZ1 content of individual samples was calculated by linear regression from the standard curves, expressed as nanograms of GSTZ1 per microgram of mitochondrial protein. All samples were measured in duplicate. The limit of quantitation (LOQ) was 0.5 ng of hGSTZ1C. Quantitation of ALDH1A1, molecular weight 55 kDa, was an estimate relative to the expression in the reference cytosol fraction, assuming a linear response to the antibody and taking into account the amount of protein in the lane.

Data analysis. To investigate possible age-related thresholds for mitochondrial GSTZ1 activity and expression, a regression-tree analysis was done, with the expression or activity as outcome and age, variants, sex and race as possible predictors. A least deviation optimization criterion was used with 15 specified as the minimum number in a node that would allow further

splitting, and 5 s the minimum number for a final node. Salford system CART was used (Salford systems, San Diego, CA). A *P* value of 0.05 was considered statistically significant.

Comparisons of GSTZ1 expression and activity in mitochondria and cytosol were analyzed by GraphPad Prism v6.0 (GraphPad Software Inc., San Diego, CA). For enzyme kinetic experiments, the kinetic parameters (V_{max}, $^{App}K_m$ and $^{App}K_{prime}$) were obtained from GraphPad Prism v6.0 by fitting the data to the Michaelis-Menten equation and the Hill equation. The best fit was determined by comparing results for the fit of each equation using Aikake's information criteria.

Michaelis-Menten equation:

$$v = \frac{V_{max} \times [S]}{K_m + [S]}$$

where V_{max} is the maximum enzyme velocity; $[S]$ is the substrate concentration; K_m is the Michaelis-Menten constant, representing the substrate concentration needed to achieve a half-maximum velocity.

Hill equation:

$$v = \frac{V_{max} \times [S]^h}{K_{prime} + [S]^h}$$

where h is the Hill slope; K_{prime} is the substrate concentration where the rate is half of V_{max}.

Time course of DCA-induced inactivation of GSTZ1. The DCA-induced GSTZ1 inactivation was assayed as previously described (Zhong et al., 2014). Human liver cytosol or sonicated mitochondria was dialyzed against 0.1 M K-phosphate buffer (pH 7.4). Dialyzed mitochondria (2 mg/mL) or cytosol (0.6 mg/mL) was incubated with 0.5 mM DCA, 5 mM GSH and 0.1 M K-phosphate (pH 7.4) in a volume of 500 μL at 37 °C for 0 – 90 min in the absence of KCl or for 0-12 hr in the presence of 38 mM KCl; control groups were those with 0 hr incubation time. Unbound substrate and product were removed by ultrafiltration after incubation, using Amicon 10 kD MWCO filters following three concentration-dilution cycles. GSTZ1 activity of

recovered protein was measured by the activity assay described above. To determine the inactivation half-life ($t_{1/2}$), the natural log of assay activity (A) divided by control activity (A_0, activity at time 0) was plotted against time. Data were fitted to the equation $\ln(A/A_0) = -k_{obs}t$ with lines forced to go through (0, 0). The $t_{1/2}$ was determined from the equation $t_{1/2} = \ln2/k_{obs}$ (Zhong et al., 2014).

Immunoprecipitation (IP) of GSTZ1. Following previously described procedures (Li et al., 2011), liver cytosol and mitochondria were obtained from 10 g of a human liver sample with GSTZ1C/1C haplotype. The mitochondrial matrix was further separated from the mitochondrial fraction. Pierce™ phosphatase inhibitor mini tablets (Thermo Fisher Scientific, Waltham, MA) were added in all the buffers used in subcellular fractionation and IP.

Procedures for IP were adapted from the manufacturer's instructions. In each batch, 10 ug rabbit polyclonal anti-hGSTZ1C was incubated with 200 μL Protein A Magnetic Beads (Bio-Rad Laboratories, Hercules, CA) and 0.1% Tween20 in phosphate buffered saline (PBS-T) with a total volume of 400 μL at 4 °C for 1 hr with rotation. Washed antibody-coupled magnetic beads were incubated with 500 μL of 5 mM bis[sulfosuccinimidyl]suberate solution freshly prepared in conjugation buffer (20 mM sodium phosphate, 0.15 M NaCl, pH 7.8), rotating at room temperature (RT) for 0.5 hr. To stop the reaction, quenching buffer (1M Tris-HCl, pH 7.5) of 25 μL was added into the incubation mixture, rotating for 15 min. After washing, beads were incubated with 100 μL of human liver cytosol or 400 μL of liver mitochondria matrix at 4 °C overnight with rotation. Unbound protein was removed and 90 μL of 20 mM glycine elution buffer pH 2.0 was added to beads to elute GSTZ1. The eluate was neutralized with 10 μL of 1M potassium phosphate buffer, pH 7.4. The procedure was repeated and several batches of eluate were combined and concentrated using 10kD MWCO filter. After concentration, samples were separated by SDS-PAGE and the gel was stained with Coomassie blue. Protein bands of cytosolic or mitochondrial GSTZ1 were cut out and stored at -80 °C for proteomic mass spectrometry analysis.

11

The analysis of protein phosphorylation by mass spectrometry. Gel bands obtained

from IP were washed with water once and then destained with a 50% acetonitrile (ACN) in 50

mM ammonium bicarbonate buffer (ABC buffer). Proteins in gel were reduced with 45 mM DTT

prepared in ABC buffer at 55 °C for 45 min, following by 45 min alkylation with 200 mM

iodoacetamide in ABC buffer at RT in the dark. Proteins were then digested with 10 ng/µL

trypsin dissolved in ABC buffer at 37 °C overnight. Peptides were extracted with 70% ACN

including 0.1% of trifluoroacetic acid (TFA) and lyophilized. Phosphopeptides were enriched

with TiO_2 NuTip micro columns (GlygenSci, Columbia MD) following the method described

previously (Gates et al., 2010).

The lyophilized peptides (enriched and flow through) were solubilized in 10 µL of loading

buffer (3% acetonitrile, 0.1% acetic acid, 0.01% TFA) and loaded onto a C18 capillary trap

cartridge (LC Packings, USA) and then separated on a 15 cm nanoflow analytical C18 column

(PepMap 75 µm id, 3 µm, 100 Å) at a flow rate of 300 nL/min on a nanoLC ultra 1D plus system

(ABsciex, USA). Solvent A composition was 3% ACN v/v, 0.1% acetic acid v/v and solvent B

was 97% ACN v/v, 0.1 % acetic acid v/v. Peptide separation was performed with a linear

gradient from 3 to 40% of solvent B for 20 min, followed by an increase to 90% of solvent B in 5

min and held for 5 min. The flow was directly sprayed to an LTQ Orbitrap-XL mass spectrometer

(ThermoFisher, Bremen, Germany). MS2 spectra were acquired in a data-dependent mode. An

Orbitrap full MS scan (resolution: 3 X 104, mass range 400–1,800 Da) was followed by 10 MS2

scans in the ion trap, which were performed via collision induced dissociation of the top 10 most

abundant ions. The isolation window for ion selection was 3 Da. Normalized collision energy

was set at 28%. Dynamic exclusion time was 20 s (Li et al., 2011). Additionally, if a phosphate

neutral loss of 98, 49, 32.66 and 24.5 m/z below the precursor ion mass was detected, there

was an additional activation. The multistage activation (MSA) event was repeated for the top

five ions in a data-dependent manner provided the precursor exceeded a threshold of 500 ion

counts (Ulintz et al., 2008). An inclusion list of the peptides for GSTZ1 N-terminal was included in the method.

Protein Search Algorithm. Tandem mass spectra were extracted by ABI Analyst (AB SCIEX, Toronto, Canada). Charge state deconvolution and deisotoping were not performed. All MS/MS samples were analyzed using Mascot (Matrix Science, London, UK; version 2.4.1). Mascot was set up to search the NCBI nr_20130403 database (selected for Homo sapiens, unknown version, 247596 entries) assuming the digestion enzyme trypsin. Mascot was searched with a fragment ion mass tolerance of 0.50 Da and a parent ion tolerance of 10.0 PPM. Carbamidomethyl of cysteine was specified in Mascot as a fixed modification. Gln->pyro-Glu of the N-terminus, deamidation of asparagine and glutamine, oxidation of methionine and phosphorylation of serine, threonine and tyrosine were specified in Mascot as variable modifications. Scaffold v4.3.4 (Proteome Software Inc., Portland, OR) was used to validate MS/MS based peptide and protein identifications. Peptide identifications were accepted if they could be established at greater than 50.0% probability by the Peptide Prophet algorithm (Keller et al., 2002) with Scaffold delta-mass correction. Protein identifications were accepted if they could be established at greater than 20.0% probability and contained at least 1 identified peptide. Protein probabilities were assigned by the Protein Prophet algorithm (Nesvizhskii et al., 2003). Proteins that contained similar peptides and could not be differentiated based on MS/MS analysis alone were grouped to satisfy the principles of parsimony. Proteins sharing significant peptide evidence were grouped into clusters.

Results

Age-related changes of GSTZ1 expression and activity in human liver mitochondria.
To determine the GSTZ1 expression level in human liver mitochondria, two GSTZ1 standard curves were constructed, with the range of 1.25 - 20 ng and 0.5-1.75 ng, respectively (Supplemental Fig.1). Among all mitochondrial samples, 101 out of 103 samples were

calculated from standard curve 1, with 5 µg of the designated human liver cytosol sample as the

reference control. The GSTZ1 contents of two mitochondrial samples were below the lower limit

of standard curve 1. Therefore, the blot was redone with longer exposure time, using 1 µg of the

designated cytosol sample as the reference control. Standard curve 2 was used to quantify

these two samples. To test if mitochondrial samples were contaminated by cytosolic proteins,

ALDH1A1 was used as a cytosolic marker on each blot to check mitochondria purity. The

intensities of ALDH1A1 bands on the blot were much lower in human liver mitochondria

compared with cytosol. Quantitation of the ALDH1A1 bands relative to the cytosol reference

showed that the mitochondrial expression was 1.59 ± 0.22% that of cytosol (mean ± S.E.M.,

n=93), indicating mitochondria had very little contamination from cytosol. A representative blot

of three samples of mitochondria is shown in Supplemental Fig. 2.

GSTZ1 expression in mitochondria was low in the first year after birth and increased with

advancing age (Fig.1A-B). GSTZ1 activity showed a similar trend (Fig.1C-D). The log scale

shown in Fig. 1B and 1D emphasizes data for the early time points. Mitochondrial GSTZ1

protein expression (Fig.2A) and enzyme activity with DCA (Fig.2B) were divided into three

groups, as indicated by the regression tree analysis, with age thresholds at 1 and 21 years old.

Median mitochondrial GSTZ1 expression increased 2-fold between the >0-1Y group and the

>1Y-21Y group and increased another 2.5- fold in the >21Y-84Y group (Fig.2A). Among

individuals of all ethnicities over 21 years old, there was no significant difference in hepatic

mitochondrial GSTZ1 expression level between GSTZ1A carriers (0.058 ± 0.034 ng GSTZ1/µg

mitochondrial protein; mean ± S.D., n=8) and non-carriers (0.060 ± 0.027 ng GSTZ1/µg

mitochondrial protein; mean ± S.D., n=38). However, mitochondrial GSTZ1 activity toward DCA

in 1A carriers (0.273 ± 0.113 nmol glyoxylate/min/mg; mean ± S.D., n=8) was significantly

higher than that in 1A non-carriers (0.109 ± 0.047 nmol glyoxylate/min/mg; mean ± S.D., n=38;

p < 0.0001), consistent with the haplotype difference observed in human liver cytosol samples

(Li et al., 2012). Significant differences for GSTZ1 expression and activity shown in Fig.2 were

determined by the non-parametric Kruskal-Wallis test with Dunn's multiple comparisons. The activity data from the thirteen 1A carriers were excluded in this analysis. A 2.7-fold increase was observed between the >0-1Y group and the >1Y-21Y group in the median GSTZ1 activity with DCA. The >21Y-84Y group increased another 2- fold (Fig.2B). Between mitochondrial GSTZ1 expression and activity, the Pearson correlation (r^2) was 0.81 for 1A carriers and 0.90 for 1A non-carriers (both p < 0.00001; Fig.3). Plots of the ratios of mitochondrial to cytosolic GSTZ1 expression (Fig.4A) and enzyme activity (Fig.4B) showed increasing trends as a function of age, with the slopes of the linear regression lines significantly larger than 0. This finding suggests that both mitochondrial GSTZ1 protein expression and GSTZ1 activity increased with age to a greater extent than their cytosolic counterparts.

Among five GSTZ1 haplotypes, GSTZ1A, 1B and 1F possess a lysine amino acid (K) at position 32 while other haplotypes have a glutamic acid amino acid (E). GSTZ1 expression data from individuals older than 21 years were analyzed by ethnicity, based on the presence of K. GSTZ1 expression in liver mitochondria was significantly lower in K carriers than in K non-carriers in Caucasians (*P < 0.01;* Table 1). This finding is consistent with previously published results showing that liver cytosolic GSTZ1 expression differed significantly between K carrier and non- carrier haplotypes in Caucasians (Langaee et al., 2015).

Properties of mitochondrial versus cytosolic GSTZ1 activity with DCA. Enzyme kinetics studies were conducted with adult human hepatic mitochondria and cytosol by separately varying GSH concentration or DCA concentration. Initial enzyme kinetic studies with GSH as the variable substrate showed the apparent K_M for GSH in human hepatic mitochondria from adults was much higher than in cytosol. We investigated the possibility that liver mitochondria consumed GSH during these assays in the absence of DCA. Studies of the stability of GSH in mitochondria showed that at low μM concentrations, a substantial proportion of the added GSH was depleted over the course of a 30 min incubation. These studies, as well as studies with cytosol, are described in detail in the next section. To calculate the apparent K_M

for GSH in mitochondria, we corrected for the loss of GSH that occurred during assays. The Hill

equation provided a better fit for the data in cytosol and in mitochondria, as assessed by

comparing the fit to that of the Michaelis-Menten equation using Aikake's Information Criteria

(Akaike, 1974) in the GraphPad software. The curves are shown in Fig 5A for cytosol and 5B for

mitochondria, and kinetic constants are presented in Table 2. The Hill coefficient was greater

than 1, indicating positive cooperativity. Similar $^{app}K'$ values were found for mitochondria and

cytosol. With DCA as the variable substrate, results from both the cytosolic and mitochondrial

forms were better fitted to the Michaelis-Menten equation (Fig.5C-D), with no significant

difference in $^{App}K_m$ values obtained from samples with GSTZ1C/1C haplotype in either

subcellular fraction (Table 3). Cytosol from 1A/1C heterozygotes showed increased $^{App}V_{max}$, as

expected, and also had significantly higher $^{App}K_m$ (Table 3). With either GSH or DCA as the

variable substrate, the $^{App}V_{max}$ values of mitochondrial GSTZ1 were significantly lower than

cytosolic GSTZ1 (Tables 2 and 3).

In the absence of chloride, both cytosolic GSTZ1 and mitochondrial GSTZ1 were

inactivated rapidly by DCA (Fig.6A; Table 4). At its physiological concentration in the whole liver

(38 mM), chloride prolonged GSTZ1 inactivation half-lives ($t_{1/2}$) 6 - 10 fold in both human liver

cytosol and mitochondria samples (Fig.6B). Inactivation half-lives of cytosolic GSTZ1 were

similar to those of mitochondrial GSTZ1 in the absence of chloride (0.54 h and 0.63 h

respectively), but 38 mM chloride protected cytosolic GSTZ1 significantly more than

mitochondrial GSTZ1. In the presence of 38 mM chloride, the inactivation half-life of cytosolic

GSTZ1 was 5.15 h and that of mitochondrial GSTZ1 was 3.83 h (*p<0.01*; Table 4).

Based on calculated yields of mitochondrial and cytosolic protein of 35 and 50 mg/g liver

respectively (Bjorntorp et al., 1965), we estimated the contribution of hepatic mitochondria and

cytosol to the initial metabolism of DCA to glyoxylate. In this estimate, we used activity data

from subjects over 21, excluding those that were heterozygous for GSTZ1A. Cytosolic activity

was 26.8 ± 16.1 nmol glyoxylate/min/g liver (mean ± S.D., n=41) and mitochondrial activity in

the same samples was 3.9 ± 1.9 nmol glyoxylate/min/g liver. Thus, assuming equal distribution of DCA throughout the liver cell, mitochondrial GSTZ1 would be responsible for 12.8% of the initial metabolism of DCA to glyoxylate. Given that DCA can enter mitochondria, its therapeutic site of action, mitochondrial GSTZ1 could play an important role in the initial metabolism of DCA.

Stability of GSH in liver cytosol and mitochondria. To explore a possible reason for the differences in GSH enzyme kinetics between cytosolic and mitochondrial GSTZ1 in human liver, we tested if GSH was consumed under conditions identical to that of the GSTZ1 activity assay, but with no addition of DCA. Mitochondria but not cytosol depleted GSH in a concentration-dependent manner over a 30 min period (Figure 7). These results were used to calculate the average concentration of GSH in studies of the apparent GSH kinetics of GSTZ1 in liver mitochondria, as noted above.

Gamma-glutamyl transpeptidase activity in liver mitochondria. GGT activity was found in adult human liver mitochondria, with linear increases in formation of *p*-nitroaniline from L-γ-glutamyl-*p*-nitroaniline occurring between 1 and 28 min. No GGT activity was detected in liver cytosol, whereas the mean mitochondrial enzyme activity was 0.67 ± 0.13 nmol/min/mg protein (n=3).

Proteomic analysis of GSTZ1. Post-translational phosphorylation of proteins can induce major changes in their function (Trost et al., 2010). To determine if phosphorylation differed in cytosolic GSTZ1and mitochondrial GSTZ1, immunoprecipitated cytosolic GSTZ1 and mitochondrial GSTZ1 were analyzed by proteomic mass spectrometry to identify phosphorylation site(s) of the protein. The sequence coverage was 64%, 65% and 72%, for cytosolic, mitochondrial and human recombinant GSTZ1C, respectively (Fig.8). The same covered sequence was shared by cytosolic and mitochondrial GSTZ1. Phosphorylated amino acids were not detected in either cytosolic or mitochondrial GSTZ1. Only one phosphorylated serine at position 188 was observed in human recombinant GSTZ1C (Fig.7; Table 5). Other

17

modifications, including Gln->pyro-Glu of the N-terminus, deamidation of asparagine and glutamine and oxidation of methionine, were similar between two forms of GSTZ1, except that asparagine (N) at position 190 was deamidated in cytosolic GSTZ1 but not in mitochondrial GSTZ1 (Table 5).

Discussion

Molecules of one protein being expressed in more than one subcellular compartment is a common phenomenon in eukaryotic cells, and is referred to as dual localization or dual targeting (Kisslov et al., 2014). Differently localized proteins, but with identical or nearly identical protein sequence, are defined as "echoforms or echoproteins." Echoforms exhibit the same or in some cases, surprisingly distinct activities and functions in each subcellular location (Raza, 2011; Yogev and Pines, 2011). Our previous studies (Li et al., 2011) have identified both mitochondria and cytosol as subcellular expression sites of GSTZ1, based on immunoreactivity, enzyme reaction and partial protein sequence (< 15%). However, the enzyme properties of liver mitochondrial GSTZ1 were incompletely understood. Considering the importance of mitochondrial GSTZ1 to DCA metabolism, we extended our investigation on mitochondrial GSTZ1 using human samples in this study. One of the aims was to investigate the developmental pattern of human liver mitochondrial GSTZ1, an important characteristic of liver cytosolic GSTZ1 in humans. Although ~99% mitochondrial proteins are encoded by nuclear genes, synthesized by the cytosolic ribosomes and translocated into mitochondria (Harbauer et al., 2014), the regulatory mechanisms of protein translocation from cytosol to mitochondria are incompletely understood. There are few studies of the relative developmental patterns of echoforms of proteins. The development of carboxylesterases 1 and 2, which exhibit microsomal and cytosolic expression, was examined in human liver samples and subtle

differences in the developmental patterns were observed (Hines et al., 2016; Boberg et al., 2017).

Our results reveal that human liver mitochondrial GSTZ1 protein expression and activity, like cytosolic GSTZ1, were directly associated with subject age. However, some differences in the developmental pattern of GSTZ1 between the two subcellular compartments were found. For example, GSTZ1 expression in human liver mitochondria reached a plateau after donor age 21 years, whereas cytosolic GSTZ1 protein expression became relatively stable after age 7 years (Li et al., 2012). The difference in age thresholds could result from different sample sizes and age distribution in the two sets of liver samples. Cytosol samples included in previously published results totaled 249, with 133 from donors > 0 - 7 years old and 55 from donors > 7-74 years old (Li et al., 2012). In contrast, in the current study, the number of liver mitochondria samples from donors > 0 - 7 years old was 28, and the other 75 samples were from donors > 7 - 84 years old. However, examination of the results for cytosolic expression of GSTZ1 in the livers used in this study showed the same developmental pattern as found previously (Li et al., 2012), i.e. protein expression reached adult levels after age 7 (Supplemental Figure 3). Of interest, the GSTZ1 expression ratio of mitochondria to cytosol, together with the GSTZ1 activity ratio, demonstrated an age-related increasing trend (Figure 4). These data indicate that the relative contribution to DCA metabolism made by mitochondrial GSTZ1, compared with cytosolic GSTZ1, increases as a function of age, even though cytosol is still the major subcellular location of DCA metabolism in cells. It is noteworthy that GSTZ1 mRNA levels do not correlate well with protein expression (Langaee et al., 2015). Further studies are needed to investigate the factors that influence the developmental pattern of GSTZ1.

There were similarities in the properties of cytosolic GSTZ1 and mitochondrial GSTZ1. Polymorphic variants exhibited the same properties for GSTZ1 activity with DCA in both locations, in that activity was significantly higher in liver samples from donors carrying the 1A variant compared with all other variants (Blackburn et al., 2000; Li et al., 2012). The difference

between the 1A variant and other variants is that the 1A variant has arginine at position 42 and

all other variants express glycine at this position, however the reason this affects activity is

unclear. Another similarity in properties between cytosolic and mitochondrial GSTZ1 was that,

as found previously for cytosolic GSTZ1 (Langaee et al., 2015), protein expression was

significantly lower in mitochondria from Caucasian individuals who carried the gene variant

coding for lysine at position 32 (variants 1A, 1B and 1F) than those who expressed glutamic

acid at this position (variants 1C and 1D). This phenomenon is due to linkage disequilibrium

between a promoter region SNP, G> A − 1002 (rs7160195), and coding region non-

synonymous SNP G>A 94 (rs7975) that occurs in Caucasians, but not Africans (our two main

ethnic groups). The $^{App}K_m$ for DCA was similar in cytosol and mitochondria from individuals with

the EGT/EGT (GSTZ1C/1C) variant. Initial studies indicated differences in the $^{App}K'$ for GSH

between mitochondria and cytosol, but further investigation showed that this was because low

concentrations of GSH were consumed by mitochondria during the course of the assay. The

finding of glutathione consumption and low GGT activity in adult human liver mitochondria was

somewhat surprising, as it has been reported that the mitochondrial pool of GSH is stable in rat

liver (Meredith and Reed, 1982). There is, however, low gene expression of GGT in adult liver

and the gene is expressed at higher levels in fetal liver (Ikeda and Taniguchi, 2005). GGT was

found on the plasma membrane of the biliary canaliculi of the hepatocyte (Hanigan and

Frierson, 1996). Plasma membrane components co-sediment with mitochondria (Suski et al.,

2014). Moreover, we did not use sucrose density gradients to isolate mitochondria, because of

the small amount of donor liver tissue available. Therefore, it is probable that contamination with

plasma membrane components is the source of GGT in our mitochondrial preparations. At

concentrations of GSH above 1 mM, within the reported physiological range of 4-10 mM (Lu,

2013), the loss of GSH over a 30 min incubation with mitochondria was very low. We did not

examine the influence of age on GSH consumption. After correcting for loss of low μM

concentrations of GSH during the GSTZ1 assay, the GSH requirements for DCA metabolism

were similar for mitochondria and cytosol. It is noteworthy that the $^{App}K'$ for GSH (less than 20

μM, Table 2) is considerably lower than the physiological concentration of GSH in either

compartment, reported to be similar in liver mitochondria and cytosol (Ribas et al., 2014).

There were differences in the properties of the two GSTZ1 echoforms. As discussed above,

the developmental profile differed. Chloride attenuation of DCA-induced GSTZ1 inactivation in

human liver cytosol was recently discovered by our group (Zhong et al., 2014), although the

mechanism is still not elucidated. This phenomenon was observed in human liver mitochondria.

In the absence of chloride, the inactivation half-lives of cytosolic GSTZ1 were similar to those of

the mitochondrial counterpart. However, the two echoforms exhibited different inactivation half-

lives of GSTZ1 in the presence of chloride, with more rapid inactivation of the mitochondrial

form. Finding GGT activity in liver mitochondria but not cytosol raised the possibility that GSH

consumption in mitochondria contributed to the faster inactivation, however, as the studies of

inactivation were carried out in the presence of 5 mM GSH, considerably higher than the

mitochondrial $^{App}K'$ for GSH, it is unlikely that the consumption of GSH by mitochondria was the

cause of this difference in the inactivation rate of GSTZ1 in the presence of chloride.

Our findings provide a plausible explanation for the observed age-related differences in

DCA pharmacokinetics and toxicity. The contribution of mitochondrial GSTZ1 to total GSTZ1

increases with age (Figure 4), so the combination of very low [Cl⁻] in mitochondria compared

with cytosol (Jahn et al., 2015) and more rapid inactivation of mitochondrial GSTZ1 (Figure 6)

suggests that the contribution of mitochondria to DCA metabolism will be quickly lost on

repeated DCA treatment.

Based on the differences between mitochondrial and cytosolic GSTZ1, we first speculated

that there may be amino acid differences in the primary protein sequences or different post-

translational modifications (e.g. phosphorylation). Multiple studies have reported that

mitochondrial protein import can be regulated by post-translational phosphorylation, for example

GSTA4, CYP2B1 and CYP2E1 (Anandatheerthavarada et al., 1999; Robin et al., 2002; Robin et

21

al., 2003). Studies by Board and co-workers identified the motif consisting of serine14, serine15 and cysteine16 as involved in GSH binding, with serine 14 as the amino acid critical for GSH binding (Board et al., 2003). Both serine 14 and 15 are potential phosphorylation sites, as well as 10 other serine residues in the GSTZ1 sequence. Our proteomic MS data, however, revealed that no difference was detected between these two echoforms of GSTZ1, either in amino acids covered in the protein sequence (>60%) or in post-translational phosphorylation. Even though cytosolic GSTZ1 possessed a deamidated Asp190, while mitochondrial GSTZ1 did not, deamidation can happen naturally during mass spectrometry sample preparation. In addition, Asp190 is relatively distant from the active site, based on the protein's crystal structure (Polekhina et al., 2001; Boone et al., 2014). As a result, it is unlikely that the deamidation status of Asp190 can lead to the differences observed between the two forms of GSTZ1.

In summary, we demonstrated an age-related increase in the expression of human hepatic mitochondrial GSTZ1, although with a different pattern to what is reported for cytosolic GSTZ1. Mitochondrial GSTZ1 activity was well correlated with GSTZ1 expression. Even though cytosolic GSTZ1 and mitochondrial GSTZ1 differed in the age-related development pattern and the half-lives of GSTZ1 inactivation in the presence of chloride, covered protein sequence and post-translational modifications, particularly phosphorylation, are identical between these two forms of GSTZ1. Low micromolar concentrations of GSH were consumed during incubation with dialyzed liver mitochondria but not with cytosol. However, this difference does not explain the developmental pattern and stability differences found between the echoforms, which are foci of future investigations.

Acknowledgements

The authors wish to thank the University of Florida Interdisciplinary Center for Biotechnology

Research for performing the proteomics mass spectrometry.

Author Contributions

Participated in research design: Zhong, James, Stacpoole, Langaee

Conducted experiments: Zhong, Smeltz, Jahn, Langaee, James

Performed data analysis: Zhong, James, Smeltz, Jahn, Langaee, Simpson

Wrote or contributed to the writing of the manuscript: Zhong, James, Stacpoole, Simpson,

Langaee, Jahn

References

Akaike, H (1974). New Look at Statistical-Model Identification. *Ieee Transactions on Automatic Control* **Ac19**(6): 716-723.

Anandatheerthavarada, HK, Biswas, G, Mullick, J, Sepuri, NB, Otvos, L, Pain, D and Avadhani, NG (1999). Dual targeting of cytochrome P4502B1 to endoplasmic reticulum and mitochondria involves a novel signal activation by cyclic AMP-dependent phosphorylation at ser128. *EMBO J* **18**(20): 5494-5504.

Bjorntorp, P, Bjorkerud, S and Schersten, T (1965). Subcellular fractionation of human liver. *Biochim Biophys Acta* **111**(2): 375-383.

Blackburn, AC, Tzeng, HF, Anders, MW and Board, PG (2000). Discovery of a functional polymorphism in human glutathione transferase zeta by expressed sequence tag database analysis. *Pharmacogenetics* **10**(1): 49-57.

Board, PG and Anders, MW (2011). Glutathione transferase zeta: discovery, polymorphic variants, catalysis, inactivation, and properties of Gstz1-/- mice. *Drug Metab Rev* **43**(2): 215-225.

Board, PG, Taylor, MC, Coggan, M, Parker, MW, Lantum, HB and Anders, MW (2003). Clarification of the role of key active site residues of glutathione transferase zeta/maleylacetoacetate isomerase by a new spectrophotometric technique. *Biochem J* **374**(Pt 3): 731-737.

Boberg, M, Vrana, M, Mehrotra, A, Pearce, RE, Gaedigk, A, Bhatt, DK, Leeder, JS and Prasad, B (2017). Age-Dependent Absolute Abundance of Hepatic Carboxylesterases (CES1 and CES2) by LC-MS/MS Proteomics: Application to PBPK Modeling of Oseltamivir In Vivo Pharmacokinetics in Infants. *Drug Metab Dispos* **45**(2): 216-223.

Boone, CD, Zhong, G, Smeltz, M, James, MO and McKenna, R (2014). Preliminary X-ray crystallographic analysis of glutathione transferase zeta 1 (GSTZ1a-1a). *Acta Crystallogr F Struct Biol Commun* **70**(Pt 2): 187-189.

Gates, MB, Tomer, KB and Deterding, LJ (2010). Comparison of metal and metal oxide media for phosphopeptide enrichment prior to mass spectrometric analyses. *J Am Soc Mass Spectrom* **21**(10): 1649-1659.

Guo, X, Dixit, V, Liu, H, Shroads, AL, Henderson, GN, James, MO and Stacpoole, PW (2006). Inhibition and recovery of rat hepatic glutathione S-transferase zeta and alteration of tyrosine metabolism following dichloroacetate exposure and withdrawal. *Drug Metab Dispos* **34**(1): 36-42.

Hanigan, MH and Frierson, HF, Jr. (1996). Immunohistochemical detection of gamma-glutamyl transpeptidase in normal human tissue. *J Histochem Cytochem* **44**(10): 1101-1108.

Harbauer, AB, Zahedi, RP, Sickmann, A, Pfanner, N and Meisinger, C (2014). The protein import machinery of mitochondria-a regulatory hub in metabolism, stress, and disease. *Cell Metab* **19**(3): 357-372.

Hines, RN, Simpson, PM and McCarver, DG (2016). Age-Dependent Human Hepatic Carboxylesterase 1 (CES1) and Carboxylesterase 2 (CES2) Postnatal Ontogeny. *Drug Metab Dispos* **44**(7): 959-966.

Hissin, PJ and Hilf, R (1976). A fluorometric method for determination of oxidized and reduced glutathione in tissues. *Anal Biochem* **74**(1): 214-226.

Ikeda, Y and Taniguchi, N (2005). Gene expression of gamma-glutamyltranspeptidase. *Methods Enzymol* **401**: 408-425.

Jahn, SC, Rowland-Faux, L, Stacpoole, PW and James, MO (2015). Chloride concentrations in human hepatic cytosol and mitochondria are a function of age. *Biochem Biophys Res Commun* **459**(3): 463-468.

Jahn, SC, Smeltz, MG, Hu, Z, Rowland-Faux, L, Zhong, G, Lorenzo, RJ, Cisneros, KV, Stacpoole, PW and James, MO (2018). Regulation of dichloroacetate biotransformation in rat liver and extrahepatic tissues by GSTZ1 expression and chloride concentration. *Biochem Pharmacol* **152**: 236-243.

James, MO, Cornett, R, Yan, Z, Henderson, GN and Stacpoole, PW (1997). Glutathione-dependent conversion to glyoxylate, a major pathway of dichloroacetate biotransformation in hepatic cytosol from humans and rats, is reduced in dichloroacetate-treated rats. *Drug Metab Dispos* **25**(11): 1223-1227.

James, MO, Jahn, SC, Zhong, G, Smeltz, MG, Hu, Z and Stacpoole, PW (2017). Therapeutic applications of dichloroacetate and the role of glutathione transferase zeta-1. *Pharmacol Ther* **170**: 166-180.

James, MO and Stacpoole, PW (2016). Pharmacogenetic considerations with dichloroacetate dosing. *Pharmacogenomics* **17**(7): 743-753.

James, MO, Yan, Z, Cornett, R, Jayanti, VM, Henderson, GN, Davydova, N, Katovich, MJ, Pollock, B and Stacpoole, PW (1998). Pharmacokinetics and metabolism of [14C]dichloroacetate in male Sprague-Dawley rats. Identification of glycine conjugates, including hippurate, as urinary metabolites of dichloroacetate. *Drug Metab Dispos* **26**(11): 1134-1143.

Kankotia, S and Stacpoole, PW (2014). Dichloroacetate and cancer: new home for an orphan drug? *Biochim Biophys Acta* **1846**(2): 617-629.

Kaufmann, P, Engelstad, K, Wei, Y, Jhung, S, Sano, MC, Shungu, DC, Millar, WS, Hong, X, Gooch, CL, Mao, X, et al. (2006). Dichloroacetate causes toxic neuropathy in MELAS: a randomized, controlled clinical trial. *Neurology* **66**(3): 324-330.

Keller, A, Nesvizhskii, AI, Kolker, E and Aebersold, R (2002). Empirical statistical model to estimate the accuracy of peptide identifications made by MS/MS and database search. *Anal Chem* **74**(20): 5383-5392.

Kisslov, I, Naamati, A, Shakarchy, N and Pines, O (2014). Dual-targeted proteins tend to be more evolutionarily conserved. *Mol Biol Evol* **31**(10): 2770-2779.

Langaee, TY, Zhong, G, Li, W, Hamadeh, I, Solayman, MH, McDonough, CW, Stacpoole, PW and James, MO (2015). The influence of human GSTZ1 gene haplotype variations on GSTZ1 expression. *Pharmacogenet Genomics* **25**(5): 239-245.

Lantum, HB, Baggs, RB, Krenitsky, DM, Board, PG and Anders, MW (2002a). Immunohistochemical localization and activity of glutathione transferase zeta (GSTZ1-1) in rat tissues. *Drug Metab Dispos* **30**(6): 616-625.

Lantum, HB, Cornejo, J, Pierce, RH and Anders, MW (2003). Perturbation of maleylacetoacetic acid metabolism in rats with dichloroacetic Acid-induced glutathione transferase zeta deficiency. *Toxicol Sci* **74**(1): 192-202.

Lantum, HB, Liebler, DC, Board, PG and Anders, MW (2002b). Alkylation and inactivation of human glutathione transferase zeta (hGSTZ1-1) by maleylacetone and fumarylacetone. *Chem Res Toxicol* **15**(5): 707-716.

Li, W, Gu, Y, James, MO, Hines, RN, Simpson, P, Langaee, T and Stacpoole, PW (2012). Prenatal and postnatal expression of glutathione transferase zeta 1 in human liver and the roles of haplotype and subject age in determining activity with dichloroacetate. *Drug Metab Dispos* **40**(2): 232-239.

Li, W, James, MO, McKenzie, SC, Calcutt, NA, Liu, C and Stacpoole, PW (2011). Mitochondrion as a novel site of dichloroacetate biotransformation by glutathione transferase zeta 1. *J Pharmacol Exp Ther* **336**(1): 87-94.

Lu, SC (2013). Glutathione synthesis. *Biochim Biophys Acta* **1830**(5): 3143-3153.

Meredith, MJ and Reed, DJ (1982). Status of the mitochondrial pool of glutathione in the isolated hepatocyte. *J Biol Chem* **257**(7): 3747-3753.

Nesvizhskii, AI, Keller, A, Kolker, E and Aebersold, R (2003). A statistical model for identifying proteins by tandem mass spectrometry. *Anal Chem* **75**(17): 4646-4658.

Polekhina, G, Board, PG, Blackburn, AC and Parker, MW (2001). Crystal structure of

maleylacetoacetate isomerase/glutathione transferase zeta reveals the molecular basis

for its remarkable catalytic promiscuity. *Biochemistry* **40**(6): 1567-1576.

Raza, H (2011). Dual localization of glutathione S-transferase in the cytosol and mitochondria:

implications in oxidative stress, toxicity and disease. *FEBS J* **278**(22): 4243-4251.

Ribas, V, Garcia-Ruiz, C and Fernandez-Checa, JC (2014). Glutathione and mitochondria.

Front Pharmacol **5**: 151.

Robin, MA, Anandatheerthavarada, HK, Biswas, G, Sepuri, NB, Gordon, DM, Pain, D and

Avadhani, NG (2002). Bimodal targeting of microsomal CYP2E1 to mitochondria through

activation of an N-terminal chimeric signal by cAMP-mediated phosphorylation. *J Biol

Chem* **277**(43): 40583-40593.

Robin, MA, Prabu, SK, Raza, H, Anandatheerthavarada, HK and Avadhani, NG (2003).

Phosphorylation enhances mitochondrial targeting of GSTA4-4 through increased affinity

for binding to cytoplasmic Hsp70. *J Biol Chem* **278**(21): 18960-18970.

Shroads, AL, Guo, X, Dixit, V, Liu, HP, James, MO and Stacpoole, PW (2008). Age-dependent

kinetics and metabolism of dichloroacetate: possible relevance to toxicity. *J Pharmacol

Exp Ther* **324**(3): 1163-1171.

Stacpoole, PW (2011). The dichloroacetate dilemma: environmental hazard versus therapeutic

goldmine-both or neither? *Environ Health Perspect* **119**(2): 155-158.

Stacpoole, PW, Gilbert, LR, Neiberger, RE, Carney, PR, Valenstein, E, Theriaque, DW and

Shuster, JJ (2008). Evaluation of long-term treatment of children with congenital lactic

acidosis with dichloroacetate. *Pediatrics* **121**(5): e1223-1228.

Stacpoole, PW, Henderson, GN, Yan, Z and James, MO (1998). Clinical pharmacology and

toxicology of dichloroacetate. *Environ Health Perspect* **106 Suppl 4**: 989-994.

Suski, JM, Lebiedzinska, M, Wojtala, A, Duszynski, J, Giorgi, C, Pinton, P and Wieckowski, MR
(2014). Isolation of plasma membrane-associated membranes from rat liver. *Nat Protoc*
9(2): 312-322.

Tate, SS and Meister, A (1977). Affinity labeling of gamma-glutamyl transpeptidase and location
of the gamma-glutamyl binding site on the light subunit. *Proc Natl Acad Sci U S A* **74**(3):
931-935.

Tong, Z, Board, PG and Anders, MW (1998). Glutathione transferase zeta-catalyzed
biotransformation of dichloroacetic acid and other alpha-haloacids. *Chem Res Toxicol*
11(11): 1332-1338.

Trost, M, Bridon, G, Desjardins, M and Thibault, P (2010). Subcellular phosphoproteomics.
Mass Spectrom Rev **29**(6): 962-990.

Tzeng, HF, Blackburn, AC, Board, PG and Anders, MW (2000). Polymorphism- and species-
dependent inactivation of glutathione transferase zeta by dichloroacetate. *Chem Res
Toxicol* **13**(4): 231-236.

Uhlen, M, Fagerberg, L, Hallstrom, BM, Lindskog, C, Oksvold, P, Mardinoglu, A, Sivertsson, A,
Kampf, C, Sjostedt, E, Asplund, A, et al. (2015). Proteomics. Tissue-based map of the
human proteome. *Science* **347**(6220): 1260419.

Ulintz, PJ, Bodenmiller, B, Andrews, PC, Aebersold, R and Nesvizhskii, AI (2008). Investigating
MS2/MS3 matching statistics: a model for coupling consecutive stage mass
spectrometry data for increased peptide identification confidence. *Mol Cell Proteomics*
7(1): 71-87.

Widdowson, EM and Dickerson, JW (1960). The effect of growth and function on the chemical
composition of soft tissues. *Biochem J* **77**: 30-43.

Yang, H, Al-Hertani, W, Cyr, D, Laframboise, R, Parizeault, G, Wang, SP, Rossignol, F,
Berthier, MT, Giguere, Y, Waters, PJ, et al. (2017). Hypersuccinylacetonaemia and

normal liver function in maleylacetoacetate isomerase deficiency. *J Med Genet* **54**(4): 241-247.

Yogev, O and Pines, O (2011). Dual targeting of mitochondrial proteins: mechanism, regulation and function. *Biochim Biophys Acta* **1808**(3): 1012-1020.

Zhong, G, Li, W, Gu, Y, Langaee, T, Stacpoole, PW and James, MO (2014). Chloride and other anions inhibit dichloroacetate-induced inactivation of human liver GSTZ1 in a haplotype-dependent manner. *Chem Biol Interact* **215C**: 33-39.

Footnotes

Portions of this work were included in Guo Zhong's Ph.D. dissertation, "Human Liver Glutathione Transferase Zeta1 (GSTZ1) in Mitochondria and Dichloroacetate-Induced GSTZ1 Inactivation, Roles of Anions, Age and Subcellular Location", located at the University of Florida Digital Collections. A preliminary report of this work was presented in September 2014 at the national meeting of the International Society for the Study of Xenobiotics.

Correspondence about this article should be addressed to Margaret O. James, Ph.D., Department of Medicinal Chemistry, P.O. Box 100485, University of Florida, Gainesville, FL 32610-0485, USA, email: mojames@ufl.edu

Figure Legends

Figure 1. Age-related changes of GSTZ1 expression (A & B) and enzyme activity with DCA (C & D) in human liver mitochondria samples. In panel A and C, data were plotted against age in years with a linear scale; the breaks in the abscissa were set at 1 year and 20 years. In panel B and D, age is shown in days with a logarithmic scale. Samples from GSTZ1A carriers are shown as red filled triangles (n=13); samples from individuals with other GSTZ1 haplotype (GSTZ1A non-carriers) are shown as open circles (n=90). Data points represent the mean of duplicate measurements.

Figure 2. Age-dependent GSTZ1 expression (A) and enzyme activity with DCA (B). The median, interquartile range and lowest to highest values of the group are shown as the horizontal bar, box, and whiskers, respectively. Outliers (black filled circles) were defined as being 1.5-fold interquartile range away from the lower or upper quartiles. The numbers below the abscissa are the number of samples. Statistical comparisons between age groups were analyzed by one-way ANOVA followed by Tukey's multiple comparisons; **$P<0.01$, ****$P<0.0001$.

Figure 3. Relationship between hepatic mitochondrial GSTZ1 expression and activity. GSTZ1A carriers are represented by red filled triangles (n=13) with a red regression line (y=3.265x+0.073); GSTZ1A non-carriers are shown as black open circles (n=90) with a black regression line (y=1.537x+0.009). Values are the means of the duplicate determinations. The slopes of three regression lines are significantly larger than 0, with the P value less than 0.0001.

Figure 4. Age-related changes in the ratios of GSTZ1 expression (A) and activity (B), between mitochondria and cytosol. Each data point is the mean value of duplicate measurements, n=103 samples. The dashed lines show linear regression with y = 0.0012x + 0.0622 (A) and y = 0.0015x + 0.1624 (B). Each slope was significantly larger than zero, $P < 0.005$.

32

Figure 5. Human liver cytosolic and mitochondrial GSTZ1 enzyme kinetics models for GSH and

DCA. Panel A, kinetic model of cytosolic GSTZ1 for GSH; panel B, kinetic model of

mitochondrial GSTZ1 for GSH; panel C, kinetic model of cytosolic GSTZ1 for DCA; panel D,

kinetic model of mitochondrial GSTZ1 for DCA. Data are shown as mean ± S.D.; black

represents samples from donors with GSTZ1C/1C haplotype; red represents samples from

donors with GSTZ1A/1C haplotype.

Figure 6. Time course of GSTZ1 inactivation by DCA in the absence (A) and presence (B) of 38

mM KCl. Data are shown as mean ± S.D.; black represents human liver mitochondria samples;

blue represents cytosol samples. All liver samples are from donors with GSTZ1C/1C haplotype.

Figure 7. Stability of various concentrations of GSH during a 30 min incubation with cytosol

(filled circles) and mitochondria (filled triangles). The concentrations of GSH shown were

incubated with 0.3 mg hepatic mitochondrial or cytosolic protein for 0 or 30 min then the

remaining GSH measured fluorimetrically following derivatization with *o*-phthalaldehyde. Points

shown are mean ± S.D. of three different liver samples.

Figure 8. Mass spectrometry analysis of protein sequence and post-translational modifications

of human liver cytosolic GSTZ1 (A), mitochondrial GSTZ1 (B) and hGSTZ1 (C). Peptide

fragments highlighted in yellow are covered by MS; amino acids highlighted in green are

modification sites.

Table 1. Human mitochondrial GSTZ1 expression related to the presence of lysine at position 32 of the protein in individuals over 21 years.

Ethnic group	GSTZ1 expression (ng GSTZ1/µg mitochondrial protein)	
	K present	K absent
Caucasians	0.038 ± 0.013 (n=11)	0.059 ± 0.013** (n=8)
Other ethnicities [a]	0.099 ± 0.024 (n=4)	0.067 ± 0.035 (n=3)

Values shown are mean ± S.D. (n).

** $P = 0.002$, significant difference between K32 carriers and non-carriers was analyzed by unpaired t test assuming equal variance

[a] The other ethnicities group included African Americans, Hispanics and others.

Table 2. Hill equation parameters of GSTZ1 enzyme kinetics for GSH.

	Cytosolic GSTZ1	Mitochondrial GSTZ1
^{App}V (pmol/mg/min)	301 ± 98	79.4 ± 13.8**
$^{App}K'$ (µM)	9.6 ± 2.6	14.5 ± 5.0
Hill coefficient	1.20 ± 0.29	1.17 ± 0.42

Data are expressed as mean ± S.D., n=4 per group

0.2 mM [1-^{14}C] NaDCA was used in incubations.

** P = 0.0148, significant difference between ^{App}V values for cytosolic GSTZ1 and mitochondrial GSTZ1, for samples with 1C/1C haplotype (paired two-tailed t test).

Table 3. Parameters of GSTZ1 enzyme kinetics for DCA

	Cytosolic GSTZ1		Mitochondrial GSTZ1
Haplotype	1C/1C (n=4)	1A/1C (n=3)	1C/1C (n=3)
$^{App}V_{max}$ (pmol/mg/min)	486 ± 122	1250 ± 372[A]	111 ± 69[B]
$^{App}K_{M}$ (µM)	26.2 ± 6.8	66.1 ± 2.4[C]	41.97 ± 14.97

Data are expressed as mean ± S.D.

GSH concentration in incubation was 1 mM for cytosolic GSTZ1 and 5 mM for mitochondrial

GSTZ1. The data fit the Michaelis-Menten model better than the Hill equation.

[A] *P = 0.002*, significant difference between haplotypes for values of cytosolic $^{App}V_{max}$

[B] *P = 0.0002*, significant difference between cytosolic and mitochondrial $^{App}V_{max}$, both with

GSTZ1C/1C haplotype, was analyzed by two-tailed *t* test assuming equal variance.

[C] *P=0.002* significant difference between haplotypes for values of cytosolic $^{App}K_{M}$.

Table 4. The influence of chloride on GSTZ1 inactivation half-lives

	Average half-lives (hr)	
	Without Cl⁻	With Cl⁻ (38 mM)
Cytosolic GSTZ1	0.54 ± 0.05	5.15 ± 0.11
Mitochondrial GSTZ1	0.63 ± 0.06	3.83 ± 0.44*

Values shown are mean ± S.D., n=3.

Cytosol and mitochondria were obtained from three human liver samples with GSTZ1C/1C

haplotype

* P = 0.02, comparing inactivation $t_{1/2}$ between cytosolic and mitochondrial GSTZ1 (paired t

test).

Table 5. Peptide sequences of GSTZ1C with post-translational modification sites

Sequence	modification	Cytosolic GSTZ1C	Mitochondrial GSTZ1C	hGSTZ1C
(M)**Q**AGKPILYSYFR(S)	Gln>Pyro-glu	Unknown	Unknown	Y
(K)DF**Q**ALNPMK(Q)	Gln>Pyro-glu[a]	N	N	Y
(K)DFQALNP**M**K(Q)	Oxidation	Y	Y	Y
(K)**Q**VPTLKIDGITIHQSLAIIEYLE E**T**RPTPR(L)	Gln>Pyro-glu[a]	N	N	Y
(R)**M**ISDLIAGGIQPLQNLSVLK(Q)	Oxidation	Y	Y	Y
(R)MISDLIAGGIQPLQ**N**LSVLK(Q)	Deamidated	N	N	Y
(R)FKVDLTPYPTIS**S**INKR	Phosphorylation	N	N	Y
(R)FKVDLTPYPTISSI**N**KR	Deamidated	Y	N	Y
(R)**Q**PDTPTELRA	Gln>Pyro-glu[a]	Y	Y	Y

Y, modification found; N, modification not found; Unknown, sequence not covered;

Underlined amino acids were modified;

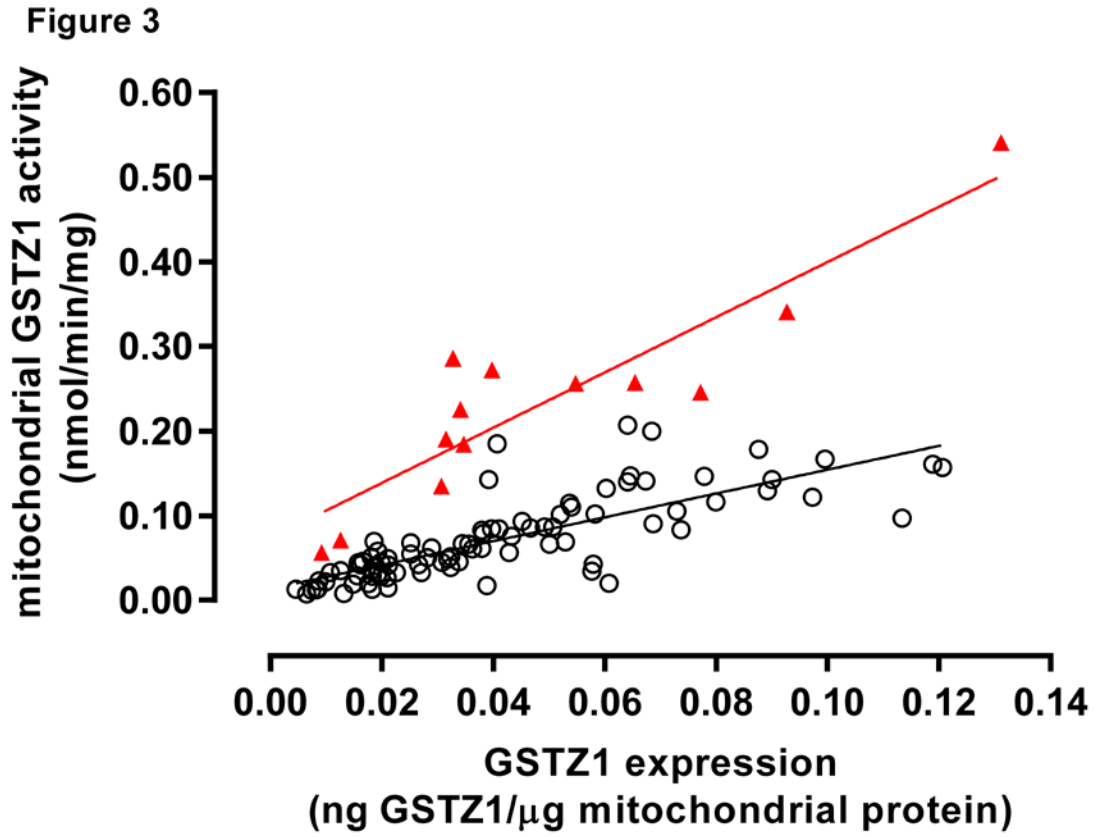[a] Pyroglutamate (Pyro-Glu) is formed from cyclization of N-terminal glutamine.
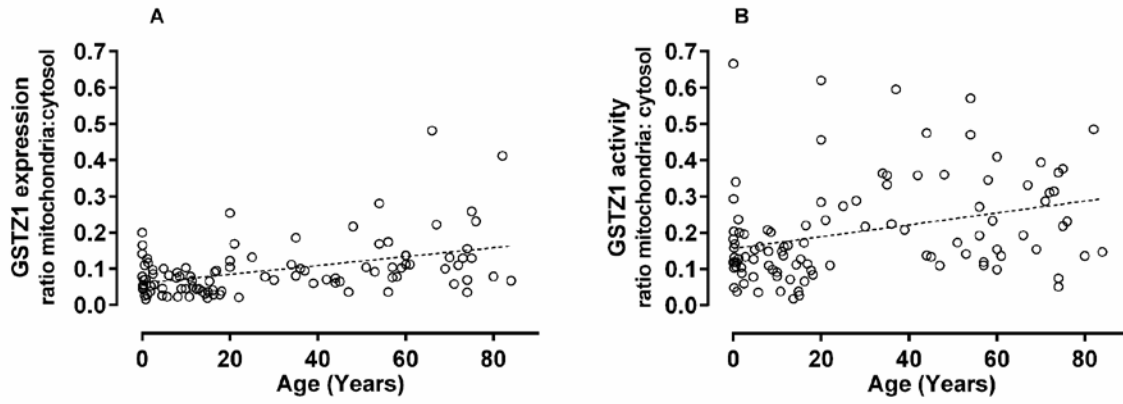
Figure 1
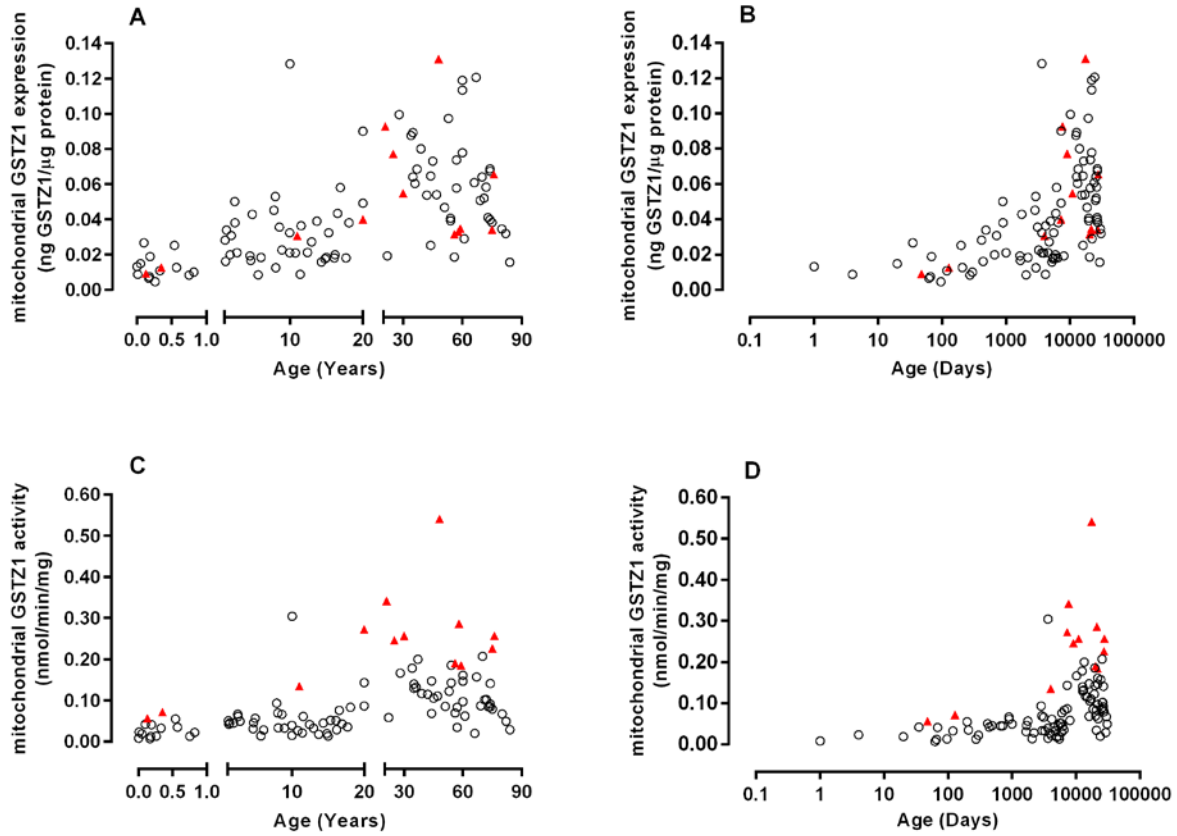
Figure 2
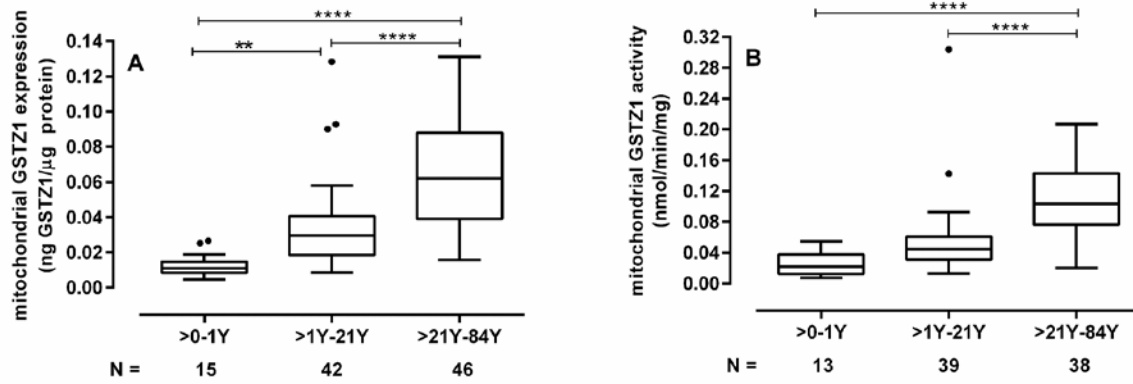
Figure 3
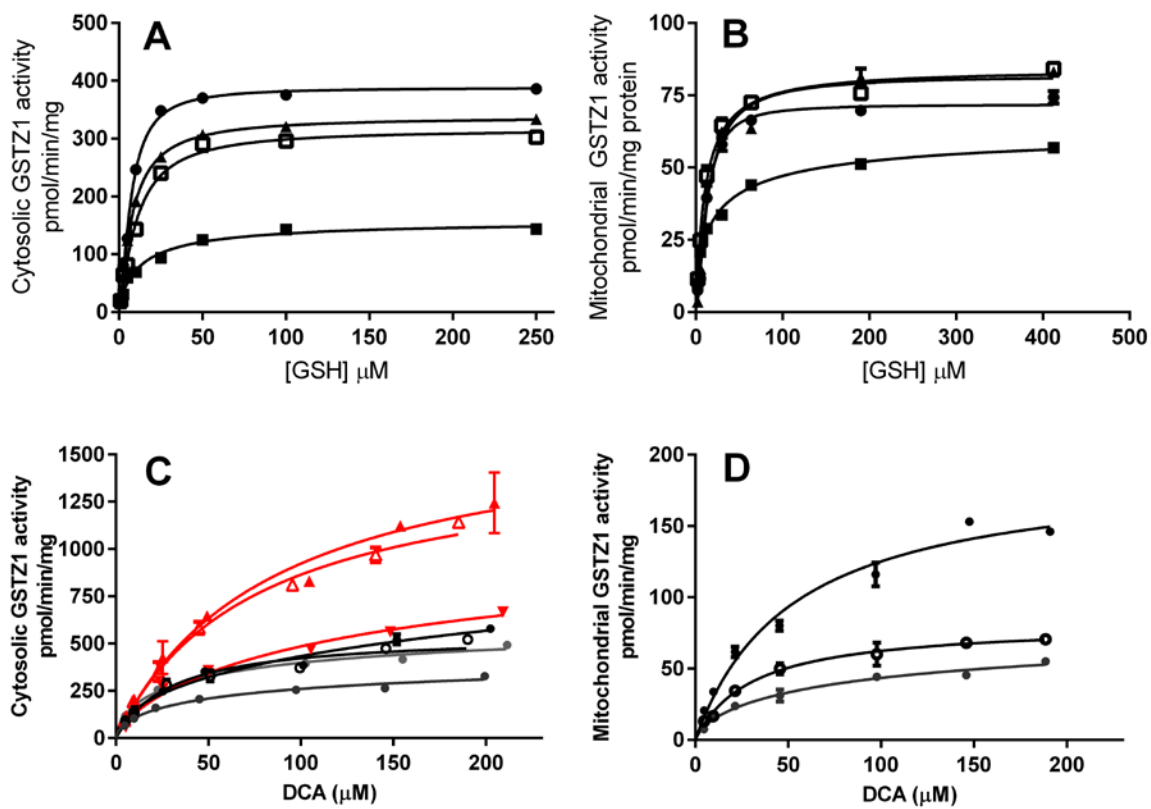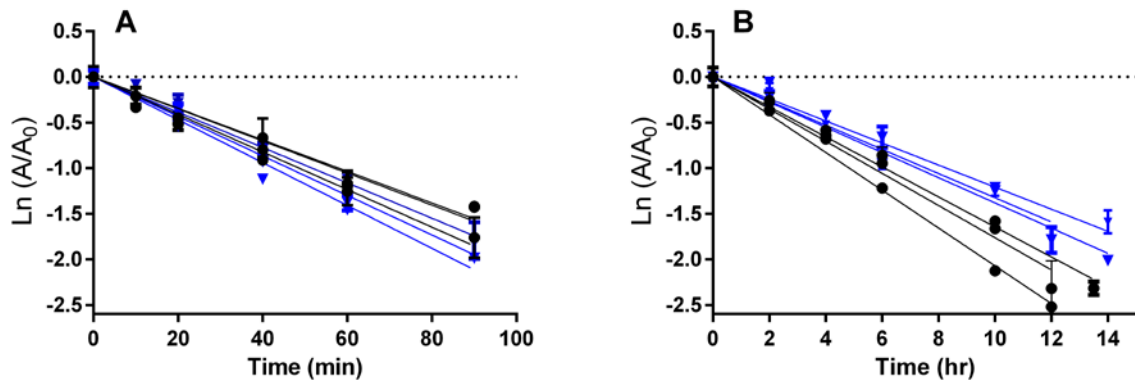
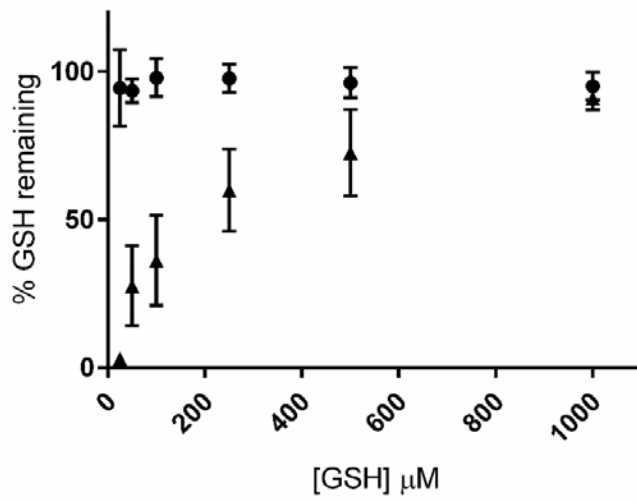## Figure 4

Figure 5

Figure 6

Figure 7

Figure 8

A

```
  1 MQAGKPILYS YFRSSCSWRV RIALALKGID YETVPINLIK DGGQQFSKDF QALNPMKQVP
 61 TLKIDGITIH QSLAIIEYLE ETRPTPRLLP QDPKKRASVR MISDLIAGGI QPLQNLSVLK
121 QVGEEMQLTW AQNAITCGFN ALEQILQSTA GIYCVGDEVT MADLCLVPQV ANAERFKVDL
181 TPYPTISSIN KRLLVLEAFQ VSHPCRQPDT PTELRA
```

B

```
  1 MQAGKPILYS YFRSSCSWRV RIALALKGID YETVPINLIK DGGQQFSKDF QALNPMKQVP
 61 TLKIDGITIH QSLAIIEYLE ETRPTPRLLP QDPKKRASVR MISDLIAGGI QPLQNLSVLK
121 QVGEEMQLTW AQNAITCGFN ALEQILQSTA GIYCVGDEVT MADLCLVPQV ANAERFKVDL
181 TPYPTISSIN KRLLVLEAFQ VSHPCRQPDT PTELRA
```

C

```
  1 MQAGKPILYS YFRSSCSWRV RIALALKGID YETVPINLIK DGGQQFSKDF QALNPMKQVP
 61 TLKIDGITIH QSLAIIEYLE ETRPTPRLLP QDPKKRASVR MISDLIAGGI QPLQNLSVLK
121 QVGEEMQLTW AQNAITCGFN ALEQILQSTA GIYCVGDEVT MADLCLVPQV ANAERFKVDL
181 TPYPTISSIN KRLLVLEAFQ VSHPCRQPDT PTELRA
```